Adv. Space Res. Vol. 10, No. 11, pp. (11)65–(11)74, 1990
Printed in Great Britain.

0273–1177/90 $0.00 + .50

DISCUSSION OF A NEW METHOD FOR MAPPING IONOSPHERIC CHARACTERISTICS

L. Bossy* and K. Rawer**

**Institut d'Aéronomie Spatiale, B-1180 Bruxelles, Belgium*
***Albert-Ludwigs-Universität, D-7800 Freiburg, F.R.G.*

ABSTRACT

For synthesizing ionospheric maps, it is proposed to use the method of "empirical orthogonal functions" instead of the inversion of the analysis schedule. For interpolating between grid points splining is not the only way. In particular, longitudinal interpolation by a low order Fourier development of the different eigenvectors components appears to be advantageous. Compared with the present synthesis method, important economies in storage capacity and computing time can be achieved.

INTRODUCTION

In 1967, CCIR /1/ adopted a station-based numerical mapping system using a combination of Fourier- and Legendre-analysis (Jones & Gallet, /2/) and a special latitude coordinate called "MODIP" (Rawer, /3/). Data analysis is executed in two steps: first Fourier-analysis station by station of the observed (monthly averaged) diurnal variation; the second step is a world-wide representation of each Fourier coefficient. For synthesis, i.e. in prediction applications, the diurnal variation at an arbitrary position is built-up by the interpolated Fourier-coefficients and this is, of course, also done at the positions of the original stations. This means that basically the same algorithm is used both for analysis and synthesis.

The CCIR-system has two major drawbacks /4/: one is the fact that large areas of the globe, in particular the oceans, have no stations. This is circumvented by an ingenious but criticizable procedure: to fill the gap, data of coastal stations are used once again at a position in the ocean obtained by "suitably shifting" it away from its original position. It was found (CCIR, /1/) that it is best achieved along the Modip coordinate /3/. Another difficulty is due to geophysical facts: the prevailing ionization processes differ over most of the Earth's surface from those over the polar cap. The reason is that there the magnetic fieldlines are open, so that corpuscles can easily arrive from the tail of the magnetosphere.

These difficulties and the analysis method will not be discussed further in the present paper. We will at present consider another method for synthesizing than the inversion of the analysis schedule used. From the analysis, we can start with a global pattern given by a set of input data at locations regularly spaced in longitude and latitude. For convenience we use a prediction map of CCIR to this end.

We apply a synthesis schedule making use of "empirical orthogonal functions". This method was invented by Pearson /5/ and was first applied in ionospheric analysis by Dvinskikh /6/. From the original (rectangular) data matrix, one constructs a square matrix, and determines its eigenvalues and eigenvectors. The approximation is then achieved using eigenvalues in order of decreasing magnitude and their corresponding eigenvectors.

* also Université Catholique de Louvain, B-1348 Louvain-la-Neuve, Belgium.

THE METHOD

A worldmap of foF2 (Figure 1) created by a rectangular matrix C of n rows and m columns; in our example m=24 (longitude) and n=60 (latitude) is used. The rows as well as the columns are independent real vectors; therefore the rank of the matrix is min(m,n). The rows are vectors in an R_n space and the columns are vectors in an R_m space; both spaces are dual. For the presentation of the method, we will admit that m<n.

The first step is to construct an m*m matrix D by

$$D = C\,C' \qquad (' \text{ indicates the transpose}) \qquad (1)$$

By its construction, D is symmetrical and positive definite; therefore all the eigenvalues of D are real and positive.

Next, we use classical methods to compute the principal components of D by:
a) first computing the m eigenvalues λ_i of D and forming an m*m diagonal matrix Λ by introducing those eigenvalues in descending order of magnitude along the diagonal;
b) second, solving the matrix equation

$$D\,U = U\,\Lambda \qquad (2)$$

where U is an orthonormal matrix with the eigenvectors $e_1, e_2, \ldots, e_m$ of D as columns. These vectors are known as the principal components of D.

Having determined U (Table 1), the Dvinskikh's method consists in expressing C as the product of U and a new m*n matrix V, such that:

$$C = U\,V \quad \text{where} \quad V = U'\,C \qquad (3)$$

The matrix V (Table 2 shows V') is formed of m row's v_i which are orthogonal n-vectors with decreasing norms. In fact, the square of the norm of each vector v_i is equal to the corresponding eigenvalue (because $V\,V' = \Lambda$). As can be seen from Table 2 the absolute values of the vector components decrease rather fast.

When, as in our applications, the magnitude of the eigenvalues decreases rapidly, this way of factorizing C is very efficient because of a property described below.

We now call

$$C_k = U_k\,V_k \quad \text{with} \quad U_k = \left| e_1, e_2, .., e_k, 0, \ldots, 0 \right| \quad \text{and} \quad V_k = \left| \begin{matrix} v_1 \\ v_2 \\ . \\ v_k \\ 0 \\ . \\ 0 \end{matrix} \right| \qquad (4)$$

the kth iterate of C.

Since: a) the sum of the squares of the elements of any real matrix A is equal to the trace of the matrix AA', b) this trace is an invariant, which becomes the sum of the eigenvalues when an orthonormal transformation is applied, c) the first k eigenvalues disappear in the trace as a consequence of the orthogonality of the eigenvectors, it follows that the elements of $C - C_k$, which are the residuals after the kth iteration of C, are such that the sum of their squares is equal to $\lambda_{k+1} + \ldots + \lambda_m$, the sum of the eigenvalues of D between k+1 and m. Therefore, the statistical variance of the residuals after the kth iteration of C equals $\lambda_{k+1} + \ldots + \lambda_m$. In our applications, this variance decreases very rapidly with increasing k.

Thus, the required accuracy will be achieved with a pth iterate, where p is the value of k for which the value of the standard deviation

$$\sigma = \sqrt{(\lambda_{p+1} + \ldots + \lambda_p)/N} \qquad (5)$$

is less than a given precision treshold ($N = m\ n$ is the total number of data). This means then that with an approximation of C by

$$C \approx C_p = U_p\ V_p \qquad (6)$$

one can reproduce the grid points of the map with maximum errors of a few σ (the majority lying between $-3\ \sigma$ and $+3\ \sigma$).

The computation of these N grid values consists in N inner products of p-vectors. These p-vectors are the first p elements in the rows of U which will be called $h(LO)$ (LO longitude) and the first p elements in the columns of V (or in the rows of the transpose) which will be called $w(LA)$ (LA latitude). (Table 3 corresponds to p less than or equal 6)

The element of C at the position LO,LA is given by the inner product

$$C(LO,LA) = (h(LO),w(LA)) \qquad (7)$$

Let $M = p\ (m+n)$ the total number of components of the matrices U_p and V_p, is the quantity of data needed for the representation of the map by the present method. Then, the ratio q between the number $N = m\ n$ of data to be represented, and M the number of data needed

$$q = N/M = (m\ n)/[p\ (m+n)] \qquad (8)$$

q can be used as a quality factor. The method saves storage as soon as q is greater than one.

FIRST APPLICATION

As said in the introduction, up to now our numerical analysis has only been carried out for one foF2-worldmap computed with the CCIR coefficients. It corresponds to March 12UT, moderate solar activity.

We thus started with $N = 24*60 = 1440$ grid-values computed for longitudes between 0 and 345° with 15° steps and latitudes from -88.5 to 88.5° with 3° steps. They constitute the well known matrix C (not reproduced).

Then, the U and V matrices were computed as Tables 1 and 2 (Table 3 was found after reduction with $p=6$). The units are respectively .001 in Table 1 and .01 Mhz in Table 2. Table 4 shows the statistical distribution of the 1440 residuals displaying for up to 24 iteration steps:

a) the variance of the residuals, i.e. the sum of their squares,
b) the maximum of the absolute values of the residuals,
c) the value of the standard deviation,
d) the distribution function of the residuals.

We see that if we want to reproduce the 1440 given data with:

high precision	Emax = .2 MHz
we need	p = 9 iterations and M = 756 inputs
good precision	Emax = .5 MHz
we need	p = 6 iterations and M = 504 inputs
poor precision	Emax = 1. MHz
we need	p = 4 iterations and M = 336 inputs

The ratios $q = N/M$ are near 2, 3, and 4 respectively.

The gain achieved by the method is limited by the most rapid changes with position on the map especially in the equatorial region.

Figure 2 shows for $p = 6$ the geographic regions where the absolute values of the residuals are above .3 MHz. This happens at some 15 grid points, all located in the equatorial region between 30°N and 30°S. It also suggests the reproduction quality one can expect with $p = 6$.

INTERPOLATION PROCEDURE

So far, we have only considered the problem of reproducing the original grid points.

In order to compete with existing procedures the method should allow easy interpolation. To this end, one should be able to compute between gridpoints e.g. between the components of each of the p eigenvectors e_i. The same should be possible among the vectors v_i. Spline interpolation is a classical means to this end.

However, we have looked for an analytical approach and tried the following:
a) because the longitude domain is normally divided in regular steps, harmonic analysis looks promising. In the present case, for the longitude LO, the kth component of h can be represented by the development

$$h_k(LO) = A_{k0} + \sum_{i=1}^{11} (A_{ki}\, C_i + B_{ki}\, S_i) + A_{k12}\, C_{12} \qquad (9)$$

where $C_i = \cos(i*LO)$ and $S_i = \sin(i*LO)$
b) because the latitude is only given in the -90°, 90° domain, harmonic development implying symmetry of the poles has been chosen such that for the latitude LA:

$$w_k(LA) = A_{k0} + \sum_{i=1}^{r} A_{ki}\, C_i \quad \text{where } C_i = \cos(i*LA) \qquad (10)$$

for k equal to 1,...,p. The coefficients occuring in this last development are computed by a least squares method and, by convention, the limiting value r of i is reached when the greatest absolute error is less than .15 MHz. For the evaluation of $h_k(LO)$ only coefficients with $i<5$ need to be retained.

INTERPOLATION IN THE ORIGINAL MAP

Applying the procedure of interpolation to the 24*60 given data and recomputing the start data using this procedure, we compared the given and recomputed values and found that a good representation (Emax reaches .51 MHz at two locations only) is obtained with 54 coefficients for the h-vectors and 146 coefficients for the w-vectors. So 200 coefficients, with a quality factor q = 7, are good enough to reproduce the grid values as accurately as with the 504 inputs needed by the Dvinskikh's method. The technique also provides an easy way for interpolating the e- and v-vectors.

Interpolating for a position LO,LA gives thus h(LO) and w(LA) and the value of C(LO,LA) at the intended location LO,LA as the inner product

$$C(LO,LA) = (h(LO), w(LA)) \qquad (11)$$

Figure 3 shows the some 30 locations where this procedure leads to absolute errors greater than .3 MHz. They are all located between 30°N and 30°S, and show no distinct structure. Emax only increases insignificantly (from .49 to .51 MHz) and there are a few more large error locations. In fact, almost all residuals fall into the noise level so that the proposed interpolation procedure causes no significant degradation of the results with the original Dvinskikh method.

FURTHER DEVELOPMENTS

Some numerical experiments were made to try to optimize the interpolation procedure.

First, we considered the effect of (regular) latitudinal spacings with 6, 9 and 12°. With p = 6, the 1440 values at the grid points were computed and compared with the original ones.

Statistical comparison gave the following results :

	Emax	Number of points with residuals > .3 MHz	Number of storages M	Value of q = N/M
6°	.46 MHz	29	193	7
9°	.56 MHz	67	174	8
12°	>2. MHz	from 60°N to 60°S		

It seems that about 10° is the maximum regular spacing permitted in latitude. With 9°, a 10% economy of storage is reached, at the cost of some loss of precision and of some spreading of the residuals towards the temperate latitudes (Figure 4). Obviously a 12° spacing cannot be satisfactory because it is unable to reproduce the equatorial and surrounding regions.

In a second series of experiments, tests with non regular spacings have been made. In particular, we have introduced a narrower spacing in the equatorial region where the variability is most important. For three schemes, the results are :

6° general spacing with 3° near the equator			
Emax = .53 MHz	33 locations	193 storages	q = 7
9° general spacing with 3° near the equator			
Emax = .60 MHz	80 locations	186 storages	q = 8
9° general spacing with 6° near the equator (Figure 5)			
Emax = .51 MHz	38 locations	186 storages	q = 8

We note that the non-regular 9° and 6° scheme is almost as good as the regular with 6° one. The more economic regular 9° scheme is less precise and shows a substantially greater number of residuals above .3 MHz. The unsatisfying result obtained with the 9° and 3° may be due to the perturbation introduced by higher orders in the Fourier decompositions; these are needed in order to reproduce the strong variations in the equatorial zone but reappear as undulating perturbations in the temperate latitudes.

CONCLUSIONS

It was the goal of this study to determine, by numerical experiments, the storage economy obtainable when establishing world maps by the Dvinskikh's method or some extension of it.

With our method of analytical interpolation, the 1440 grid points used for the definition of the map could satisfyingly be recomputed with only 175 to 200 storages, thus with a quality factor between 7 and 8. At a few locations, in the equatorial region, the residuals went up to ≈ .5 MHz. Our procedure also allows to interpolate in the map with no significant loss of precision. The original Dvinskikh's method gives a representation which is slightly better but needs follow-up local interpolations. Some 500 storages are necessary, leading to a quality factor of only 3. Thus, the introduction of descriptive functions in place of the original discrete values of the elements of the e- and v-vectors is advantageous.

There is, of course, no unique way of looking for such interpolation functions. They have to be chosen having in mind the type of map considered : worldmap or regional map.

The good results reported have perhaps been influenced by the fact that the grid data were derived from a smooth Legendre expansion without noise.

ACKNOWLEDGMENTS

This work was in part supported by Fonds National de la Recherche Scientifique-Crédits aux Chercheurs.

BIBLIOGRAPHY

1) Comité Consultatif International des Radiocommunications (CCIR), CCIR Atlas of ionospheric characteristics, Report 340, Geneva (1967 and last revision 1983)

2) W.B. Jones and R.M. Gallet, The representation of diurnal and geographical variation of ionospheric data by numerical methods, ITU Telecomm. J. 29, 129-149 (1962) and 32, 18-28 (1965)

3) K. Rawer, Propagation of decameter waves (HF band), in: Meteorological and Astronomical Influences on Radio Wave Propagation, ed. B. Landmark, Academic Press, New York, 221-250 (1963)

4) K. Rawer, The historical development of forecasting methods for ionospheric propagation of HF waves, Radio Sc. 10, 7, 669-679 (1975)
Ionospheric modelling during the last decades, Ind. J. Radio & Space Phys. 15, 217-234 (1986)

5) K. Pearson, On lines and planes of closest fit to systems of points in space, Phil. Mag. 6, 559-572 (1901)

6) N.I. Ovinskikh, Expansion of ionospheric characteristic fields in empirical orthogonal functions, Adv. Space Res. 8, 4, 179-187 (1988)

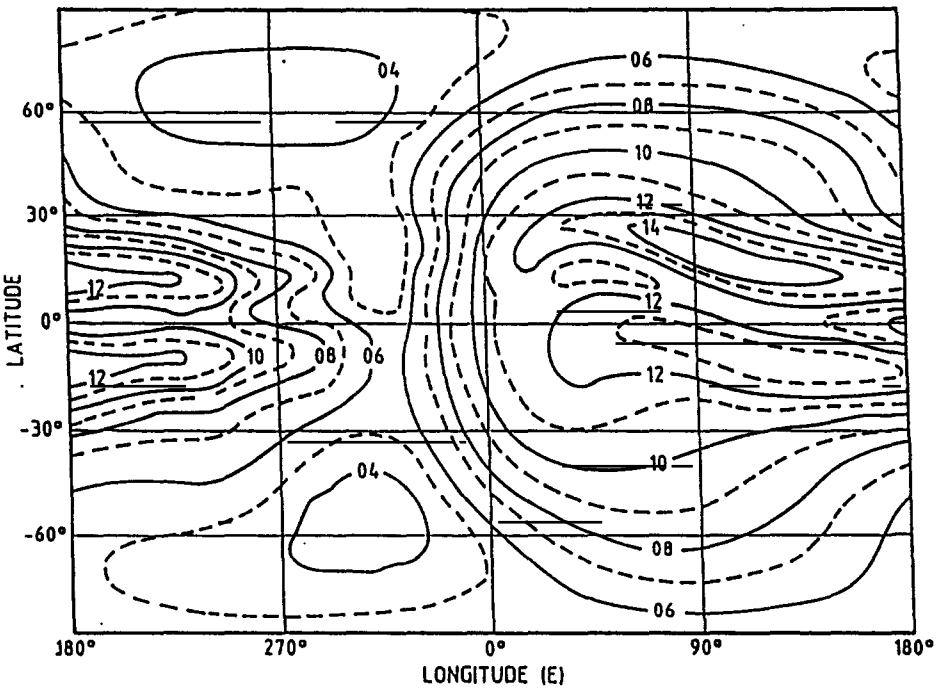

Fig. 1. Worldmap of foF2.

217	97	21	55	312	497	105	13	146	6	213	106	53	72	370	399	8	17	232	152	62	104	134	236
236	170	80	41	228	358	-353	166	-291	-310	165	337	-94	54	-277	-164	-29	32	-251	-4	13	-31	-173	-140
245	239	9	178	229	-138	-197	51	-451	143	-381	-386	-127	266	146	73	155	-95	12	-122	-38	-32	214	-24
249	278	-50	265	215	-351	170	-235	-118	141	455	-28	384	-237	-216	13	-144	-115	-23	-29	-20	-20	55	-10
251	302	-18	284	-25	-339	105	30	311	64	-39	271	-588	-14	110	-17	55	207	20	116	36	44	-189	26
252	279	67	140	-383	-72	-77	299	279	-254	-231	74	576	190	99	-15	54	24	0	-16	12	2	-12	-7
252	185	161	-112	-520	187	-112	75	-94	40	23	-160	-265	-410	-149	141	-277	-288	170	14	-70	0	121	79
250	75	186	-249	-269	128	5	-339	-165	195	136	-50	69	-88	188	-238	318	512	-173	-93	156	5	32	77
244	-2	174	-274	-17	-23	148	-359	5	-106	49	-9	-16	307	194	-205	33	-396	160	310	-259	38	-185	-283
235	-60	164	-285	87	-102	293	-71	58	-193	-56	-19	-92	310	-226	109	-228	-54	43	-474	348	-119	-70	272
225	-122	150	-283	131	-123	285	210	-1	-10	-171	35	11	-7	-277	193	-114	318	-254	323	-287	75	297	-165
211	-193	111	-229	207	-165	2	239	6	67	-140	153	82	-478	156	124	437	-336	-105	-85	178	102	-221	-45
198	-255	64	-115	203	-209	-343	110	84	-75	62	24	32	-175	312	-230	-313	213	294	-136	-228	-394	249	95
187	-291	44	9	27	-151	-415	9	104	150	79	-122	40	164	-216	-121	-88	37	166	236	226	605	-300	112
182	-312	61	154	-176	34	-178	31	96	411	166	-51	17	254	-70	381	32	-45	-229	119	66	-461	21	-53
179	-338	49	314	-111	81	42	-59	178	-116	180	31	-130	66	-29	-33	222	-97	-102	-511	-379	224	155	-196
170	-309	-42	349	-16	36	97	-240	-7	-477	-152	-176	-51	-192	-22	-177	65	-39	-76	346	363	-226	265	70
154	-222	-147	208	-75	90	112	-241	-291	28	-368	164	137	-129	124	182	-294	136	-59	-75	-269	209	-476	167
142	-156	-213	79	-118	102	241	149	-250	281	-101	386	48	69	-142	-189	33	27	493	-10	242	-69	196	-291
131	-111	-306	-25	-112	-2	278	430	-179	59	247	-99	-61	138	152	-360	0	-167	-234	111	-119	-31	-34	446
114	-25	-466	-171	-115	-110	4	132	-121	-313	279	-300	-67	-11	167	309	-10	223	72	-55	121	157	-208	-411
112	57	-525	-261	-49	-88	-253	-277	67	-95	-77	220	1	48	-279	152	326	-60	105	34	-219	-172	191	333
141	80	-376	-142	72	132	-104	-158	284	221	-183	69	-1	-32	187	-167	-372	-183	-432	-94	211	71	164	-255
183	74	-146	26	226	350	136	69	346	149	-162	-459	37	-151	-308	-221	131	128	171	-54	-148	-80	-228	-33

TABLE 1 Elements of Matrix U (in .001).

2559	-265	-471	-34	-28	54	-4	17	0	3	-3	4	-1	6	-2
2586	-197	-406	-52	-35	34	-3	10	7	3	-2	2	0	3	-1
2617	-129	-344	-65	-46	13	-3	3	13	2	-2	0	-1	1	0
2650	-63	-284	-73	-58	-7	-1	-3	17	2	-3	0	0	-2	0
2685	-1	-223	-72	-69	-29	0	-10	16	0	-3	1	0	-4	1
2725	52	-163	-62	-79	-47	1	-17	10	-2	-1	2	0	-4	2
2774	96	-108	-42	-87	-60	0	-24	3	-4	0	4	0	-4	2
2832	131	-60	-16	-91	-67	-1	-31	-2	-5	1	5	0	-2	1
2900	158	-21	9	-92	-68	-4	-37	-9	-6	1	7	0	-1	1
2978	178	7	39	-90	-63	-8	-43	-15	-7	2	8	0	0	0
3069	194	24	68	-82	-51	-12	-49	-19	-6	1	7	0	1	0
3168	204	30	94	-70	-53	-16	-53	-22	-5	0	7	0	2	0
3277	211	25	115	-54	-9	-21	-55	-22	-3	-1	5	0	2	-1
3393	214	11	130	-33	17	-25	-55	-20	-1	-2	2	0	1	-1
3517	211	-8	137	-8	44	-29	-52	-17	1	-3	0	1	1	-2
3645	202	-32	136	17	68	-33	-47	-14	3	-4	-3	0	0	-1
3780	185	-57	127	45	84	-35	-38	-12	5	-5	-6	1	-1	0
3922	156	-78	108	72	91	-37	-26	-13	5	-3	-6	5	-3	-6
4074	114	-93	82	97	85	-40	-12	-15	5	-1	-6	1	-2	1
4241	50	-95	48	117	66	-42	3	-20	2	1	-3	0	-2	3
4429	-37	-83	11	130	30	-45	18	-27	0	4	0	0	-1	4
4643	-159	-54	-23	134	-18	-49	31	-34	-2	7	3	0	0	3
4886	-312	-10	-46	122	-72	-50	37	-39	-4	8	4	0	1	2
5145	-484	38	-49	92	-117	-42	34	-39	-5	6	1	0	2	0
5389	-631	72	-25	42	-134	-18	22	-37	-3	0	-3	0	0	-3
5551	-685	67	23	-22	-106	27	8	-34	1	-9	-10	1	-1	-5
5562	-577	12	83	-90	-37	80	1	-34	6	-12	-12	1	-2	-1
5398	-326	-61	133	-132	33	106	13	-31	5	-2	-6	1	0	4
5155	-76	-96	168	-114	57	79	32	-9	-14	15	0	-1	2	5
4993	-13	-53	197	-34	28	19	37	34	-40	20	0	-2	0	0
5009	-195	36	210	74	-15	-14	17	74	-40	2	0	0	-3	-4
5166	-498	121	155	152	-32	7	-18	82	-9	-17	2	0	0	0
5339	-728	196	6	153	-4	47	-52	53	22	-9	6	-2	4	4
5417	-762	280	-164	61	67	49	-59	13	24	16	7	-4	0	0
5371	-583	364	-245	-77	136	-1	-20	-4	-2	17	3	4	-4	-5
5252	-253	404	-183	-175	133	-55	38	5	-20	-10	1	3	3	0
5080	94	368	-42	-154	56	-63	51	2	7	-11	1	-26	-2	0
4902	395	284	94	-118	-33	-45	67	26	17	-14	3	7	5	4
4676	548	177	138	-45	-61	-9	48	23	33	4	3	4	0	-1
4452	601	81	110	9	-37	18	34	15	31	12	3	2	-2	-4
4259	604	10	50	45	4	36	26	5	19	10	1	1	-1	-3
4107	591	-30	-10	66	33	46	22	-3	6	3	2	-1	0	-2
3987	575	-46	-60	77	45	50	18	-11	-3	-2	2	-1	1	0
3882	557	-41	-98	80	40	50	14	-15	-9	-6	2	-1	1	0
3779	535	-23	-123	78	24	45	9	-16	-12	-8	2	-1	0	0
3666	509	0	-141	69	4	37	4	-12	-13	-8	2	0	0	0
3542	479	25	-152	58	-15	28	-2	-5	-12	-8	0	0	0	0
3402	446	45	-156	43	-32	17	-8	1	-10	-5	-1	0	-1	0
3250	410	54	-153	27	-44	8	-14	9	-6	-3	-3	0	0	0
3089	372	52	-145	10	-49	0	-19	17	-4	0	-6	0	0	0
2926	329	33	-131	-4	-49	-7	-23	22	-1	3	-8	0	0	0
2769	280	0	-113	-18	-42	-12	-25	24	0	5	-9	0	3	0
2627	223	-45	-91	-30	-32	-17	-24	26	2	8	-10	0	4	0
2512	155	-100	-70	-38	-20	-21	-21	25	4	10	-10	-1	5	0
2433	71	-159	-57	-40	-10	-25	-15	23	6	10	-8	0	4	0
2401	-28	-214	-55	-34	-8	-28	-1	23	8	6	-4	0	-1	1
2411	-134	-263	-66	-23	-10	-27	15	22	9	-1	2	3	-11	2
2427	-213	-320	-63	-25	0	-18	17	18	7	-4	4	1	-4	-1
2435	-258	-383	-51	-30	22	-9	15	9	5	-4	5	0	1	-2
2431	-279	-447	-33	-28	47	-4	16	1	4	-4	4	-1	5	-3

TABLE 2 Elements of the Transpose of Matrix V (9 last columns omitted).

217	97	21	55	312	497
236	170	80	41	228	358
245	239	9	178	229	-138
249	278	-50	265	215	-351
251	302	-18	284	-25	-339
252	279	67	140	-383	-72
252	185	161	-112	-520	187
250	75	186	-249	-269	128
244	-2	174	-274	-17	-23
235	-60	164	-285	87	-102
225	-122	150	-283	131	-123
211	-193	111	-229	207	-165
198	-255	64	-115	203	-209
187	-291	44	9	27	-151
182	-312	61	154	-176	34
179	-338	49	314	-111	81
170	-309	-42	349	-16	36
154	-222	-147	208	-75	90
142	-156	-213	79	-118	102
131	-111	-306	-25	-112	-2
114	-25	-466	-171	-115	-110
112	57	-525	-261	-49	-88
141	80	-376	-142	72	132
183	74	-146	26	226	350

2559	-265	-471	-34	-28	54
2586	-197	-406	-52	-35	34
2617	-129	-344	-65	-46	13
2650	-63	-284	-73	-58	-7
2685	-1	-223	-72	-69	-29
2725	52	-163	-62	-79	-47
2774	96	-108	-42	-87	-60
2832	131	-60	-16	-91	-67
2900	158	-21	9	-92	-68
2978	178	7	39	-90	-63
3069	194	24	68	-82	-51
3168	204	30	94	-70	-53
3277	211	25	115	-54	-9
3393	214	11	130	-33	17
3517	211	-8	137	-8	44
3645	202	-32	136	17	68
3780	185	-57	127	45	84
3922	156	-78	108	72	91
4074	114	-93	82	97	85
4241	50	-95	48	117	66
4429	-37	-83	11	130	30
4643	-159	-54	-23	134	-18
4886	-312	-10	-46	122	-72
5145	-484	38	-49	92	-117
5389	-631	72	-25	42	-134
5551	-685	67	23	-22	-106
5562	-577	12	83	-90	-37
5398	-326	-61	133	-132	33
5155	-76	-96	168	-114	57
4993	-13	-53	197	-34	28
5009	-195	36	210	74	-15
5166	-498	121	155	152	-32
5339	-728	196	6	153	-4
5417	-762	280	-164	61	67
5371	-583	364	-245	-77	136
5252	-253	404	-183	-175	133
5080	94	368	-42	-154	56
4902	395	284	94	-118	-33
4676	548	177	138	-45	-61
4452	601	81	110	9	-37
4259	604	10	50	45	4
4107	591	-30	-10	66	33
3987	575	-46	-60	77	45
3882	557	-41	-98	80	40
3779	535	-23	-123	78	24
3666	509	0	-141	69	4
3542	479	25	-152	58	-15
3402	446	45	-156	43	-32
3250	410	54	-153	27	-44
3089	372	52	-145	10	-49
2926	329	33	-131	-4	-49
2769	280	0	-113	-18	-42
2627	223	-45	-91	-30	-32
2512	155	-100	-70	-38	-20
2433	71	-159	-57	-40	-10
2401	-28	-214	-55	-34	-8
2411	-134	-263	-66	-23	-10
2427	-213	-320	-63	-25	0
2435	-258	-383	-51	-30	22
2431	-279	-447	-33	-28	47

TABLE 3 Matrices U and Transposed V as Used for Numerical Experiments (U in .001 and V in .01 MHz).

p	Variance	E_m	σ	Frequencies
01	1145.8253	303	892	0 0 12 87 302 617 314 98 10 0 0
02	348.9192	251	492	0 2 14 33 347 667 299 45 16 14 0
03	143.8461	156	316	1 3 9 71 370 558 333 85 8 2 0
04	75.7184	119	229	1 3 14 77 272 678 317 56 18 2 2
05	37.9637	76	162	1 6 10 82 276 661 321 66 14 2 1
06	18.8878	49	115	0 2 23 69 302 648 302 83 9 2 0
07	11.3185	41	89	1 3 19 62 304 661 292 82 14 2 0
08	5.5777	40	62	4 3 17 64 252 772 256 51 12 6 3
09	1.7410	20	35	3 7 14 42 268 785 255 39 15 6 6
10	.7720	17	23	3 1 15 59 307 680 315 40 10 7 3
11	.3958	16	17	3 1 6 66 284 710 309 47 6 4 4
12	.2277	15	13	3 2 8 40 269 797 281 29 6 0 6
13	.1203	8	9	0 4 17 58 300 673 308 67 10 1 2
14	.0636	3	7	0 2 14 75 278 682 293 77 16 2 1
15	.0275	3	4	1 6 11 64 264 752 250 72 15 2 3
16	.0103	2	3	2 3 13 64 270 717 290 66 11 2 2
17	.0046	1	2	0 5 14 64 301 680 293 67 12 3 1
18	.0027	1	1	1 7 15 58 279 732 253 74 17 4 0
19	.0016	1	1	0 4 19 68 250 759 254 64 17 5 0
20	.0013	0	1	1 2 19 70 267 723 266 74 14 3 1
21	.0009	0	1	2 4 17 61 255 757 259 62 16 5 2
22	.0006	0	1	2 5 15 66 240 779 248 60 18 6 1
23	.0005	0	1	1 4 22 53 270 737 281 47 15 9 1
24	.0002	0	0	1 6 16 55 268 745 268 58 16 5 2

TABLE 4 p: order of the iteration. Variance: sum of the squares of the residuals (in MHz^2). Column E_m: maximum absolute value amongst the residuals (in .01 MHz). Column σ: standard deviation in (.001 MHz). Last 11 columns: statistical distribution of the deviations central column around zero (i.e. in $-\frac{1}{2}\sigma$ and $\frac{1}{2}\sigma$), side columns for larger deviations (in $1.\sigma$ steps).

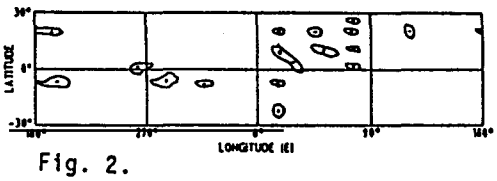

Fig. 2.

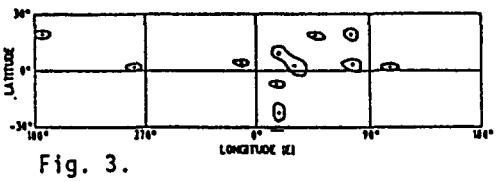

Fig. 3.

Fig. 2. Geographical distribution of the locations giving absolute errors greater than .3 MHz (dots identify error peaks) with Dvinskikh's original method (latitudinal spacing 3°, 540 coefficients), for p = 6.

Fig. 3. Same as Figure 2 when the Fourier interpolation method (with 200 coefficients) is applied (p = 6).

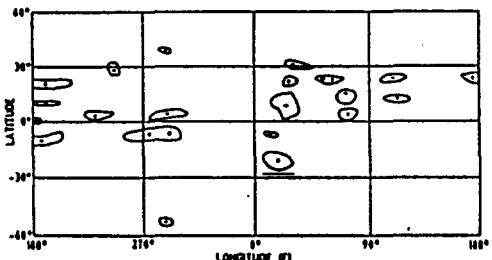

Fig. 4.

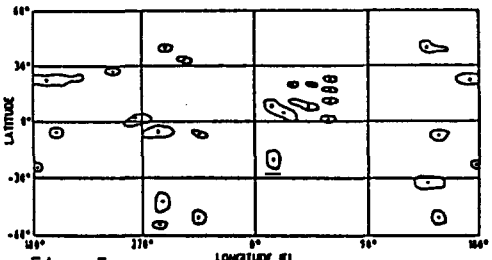

Fig. 5.

Fig. 4. Same as Figure 3 for 9° regular spacing (p = 6).

Fig. 5. Same as Figure 3 for 9° and 6° adopted spacing (p = 6).